PERFORMANCE INVESTIGATION OF A DUAL-SOURCE HEAT PUMP FOR A SWINE NURSERY BARN IN NORTHERN ITALY

George Meramveliotakis[1*], Dimitrios Tyris[2*], Apostolos Gkountas[3], Panteleimon Bakalis[3], Stefano Benni[4], Francesco Tinti[5], Dimitris Manolakos[2]

[1]THERMODRAFT IKE, Piraeus, Greece

[2]Agricultural University of Athens, Department of Natural Resources Development and Agricultural Engineering, Athens, Greece

[3]PSYCTOTHERM, Piraeus, Greece

[5]University of Bologna, Department of Agricultural and Food Sciences, Bologna, Italy

[4]University of Bologna, Department of Civil, Chemical, Environmental, and Materials Engineering, Bologna, Italy

*Corresponding Author: gmeramveliotakis@thermodraft.gr, dtyris@aua.gr

ABSTRACT

Achieving carbon neutrality relies on decarbonizing the heating of the building sector and heat pumps (HPs) possess significant potential to substitute non-renewable heating equipment. To address the application difficulties encountered by conventional heat pumps, there is a growing focus on the adoption of dual-source heat pumps (DSHP), which are potentially both more efficient and versatile. The present study highlights the development and experimental testing of a novel DSHP with digital capacity modulation. This system is designed to replace an LPG (Liquified Petroleum Gas) boiler for space heating in a swine burn, marking a significant exploration into the utilization of heat pumps in livestock buildings, an area that has received relatively limited attention in previous research. Specifically, HP's performance is analyzed based on the pre-operational testing procedure and Seasonal Coefficient of Performance (SCOP) is calculated, according to EN-14825. Results reveal that DSHP operation achieves heating capacities of 30-32 kW with a COP approaching 5 in water-source mode, while in air-source mode, heating capacities exceed 30 kW with a COP ranging from 3-4. Hybrid operation demonstrates a modest improvement in COP alongside a 25% increase in heating capacity compared to air source mode. Additionally, with digital capacity modulation activated, the heat pump is tested in various compressor capacity modes (ranging from 20-100%) providing valuable insights into the performance of the system.

1 INTRODUCTION

Despite accounting for 46% of global final energy consumption, buildings still heavily rely on fossil energy for heating, contributing to 40% of global carbon emissions (Pilou et al., 2023). Renewable heating devices, particularly heat pumps, are gaining momentum, supported by governmental initiatives and ongoing research. Heat pumps, as highly efficient electric devices, offer a versatile solution for heating, cooling, and domestic hot water (DHW) production. Hybrid systems, incorporating both ground and air as heat sources, offer cost advantages and increased seasonal performance (Meramveliotakis et al., 2020). The dual-source heat pump (DSHP), integrating water and air sources directly into the design, proves to be a compact, energy-efficient, and cost-effective alternative (Corberán et al., 2018). Researchers have demonstrated the effectiveness of DSHPs in improving performance factors compared to systems relying solely on groundwater or air sources. Li et al. (2023) conducted a comparison between the conventional HP heating system and the DSHP system in various Chinese regions. The results showed a reduction in annual heating bills and carbon emissions ranging from 1.88% to 21.53%. Additionally, the experimental investigation by Han et al. (2017) on a multi-

https://doi.org/10.52202/077185-0090

source HP revealed that with the implementation of the collector/evaporator system, the average heat capacity and COP of the unit increased by 5.14% and 4.90% respectively, compared to a common HP, under varying solar radiation intensities. Grossi et al. (2018) tested and compared a novel DSHP system (utilizing air and ground heat sources) with an Air Source Heat Pump (ASHP) through annual simulations. The results indicated that the DSHP system achieved a superior annual performance of 24.6% compared to ASHP and demonstrated more stable performance over the years. Wang et al. (2021) developed a dual-source heating system that extracts energy from both a photovoltaic/thermal water heat exchanger and an air heat exchanger. This system reduced heating costs by 45% and operated more stably when compared to an ASHP heating system. Moreover, Marinelli et al. (2020) indicated that a DSHP air/ground system is more environmentally friendly than both a conventional ASHP solution in humid climates and a Ground Source Heat Pump (GSHP) system since it requires shorter geothermal probes for the Borehole Heat Exchangers (BHE). This paper focuses on the pre-operational testing of a DSHP for livestock buildings, an environment in which HPs have not been widely studied theoretically in current literature or applied. Its main characteristics and components are analyzed, and the methodology to determine its SCOP according to EN 14825 (DIN, 2016) is explained and evaluated. To investigate the impact of different control options, the operation of the DSHP heat pump in different compressor capacities for both the water- and air-source modes, as well as hybrid operation are presented and compared. Moreover, the performance of its digital capacity operation for the abovementioned modes is highlighted.

2 SYSTEM DESIGN AND DESCRIPTION

An efficient and flexible dual-source heat pump (air/water-to-water) has been designed and manufactured, to be installed in a commercial swine farm, located in Northern Italy, to cover the heating needs of its nursery barn. The HP is designed to substitute the existing 35 kW LPG boiler, operating at medium temperatures (hot water outlet up to 45 ^{o}C) achieving a high Coefficient of Performance (COP). This design is based on a flexible modular configuration that can exactly address the buildings' needs and exploit both ambient heat, and heat flowing from a Photovoltaic/ Thermal (PVT) system to the heat pump, through a Borehole Thermal Energy Storage (BTES) system, ensuring cost-effectiveness, low complexity, and low maintenance needs.

2.1 System Design and Cycle Parameters

The basic system design integrates a dual-source heat pump which, besides an air-heated evaporator, also includes a heat exchanger to exchange heat with a water/ glycol mixture from a series of PVT collectors, coming through the boreholes. The designed Borehole Thermal Energy Storage (BTES) system comprises eight 30-meter double-U Borehole Heat Exchangers (BHEs), configured into two circuits with four lines. Each BHE is fully utilized, with its double-U structure divided between the heat pump (HP) and the PVT lines.

The main innovation of the system lies in the possibility of hybrid operation, utilizing at the same time both the available heat from the ground and the air, leading to enhanced heating capacity and COP. Focusing on the heat pump, the selected refrigerant is the HFC blend R407C, which presents similar properties with common refrigerant HCFC-22 under evaporator temperatures in the range from –7 to 10 °C, showing zero ozone depletion potential (ODP). The components were selected based on the system's specifications, to cover the worst possible operating conditions. For evaporation and condensation temperatures of 13 °C and 55 °C respectively, the cycle parameters are the typical ones applied in standard heat pump units. More specifically the design parameters are:

- Superheat at the compressor suction and subcooling at the economizer outlet of 10 K and 5 K respectively.
- Pinch point temperature difference at the evaporator and condenser of 3 K.
- The water (water/glycol in the evaporator) temperature difference between the inlet and outlet at the evaporator and condenser is 2 and 3 K, respectively.

Regarding the water/ glycol design flowrates, Table 1 provides information about the properties at the reference conditions of 20/55 °C for the evaporator and condenser side.

https://doi.org/10.52202/077185-0090

Table 1: Properties for the cold/hot side of the HP.

Water/ glycol flow	Temperature (°C)	Pressure (bar)	Flowrate (m^3/h)
Evaporator (in / out)	20 / 15	2 – 4	6.4
Condenser (in / out)	45 / 55	2 – 4	3.9

2.2 Components Selection

Based on the cycle parameters, the heat pump's components were selected accordingly, to cover the least favorable operating conditions for the application. The selection of components is a critical activity of the whole design process and mainly focuses on the heat exchanger (HEX) sizing, which should operate with a low enough pinch point even in off-design conditions. The components are presented below with the schematic diagram of the tested heat pump shown in Figure 1.

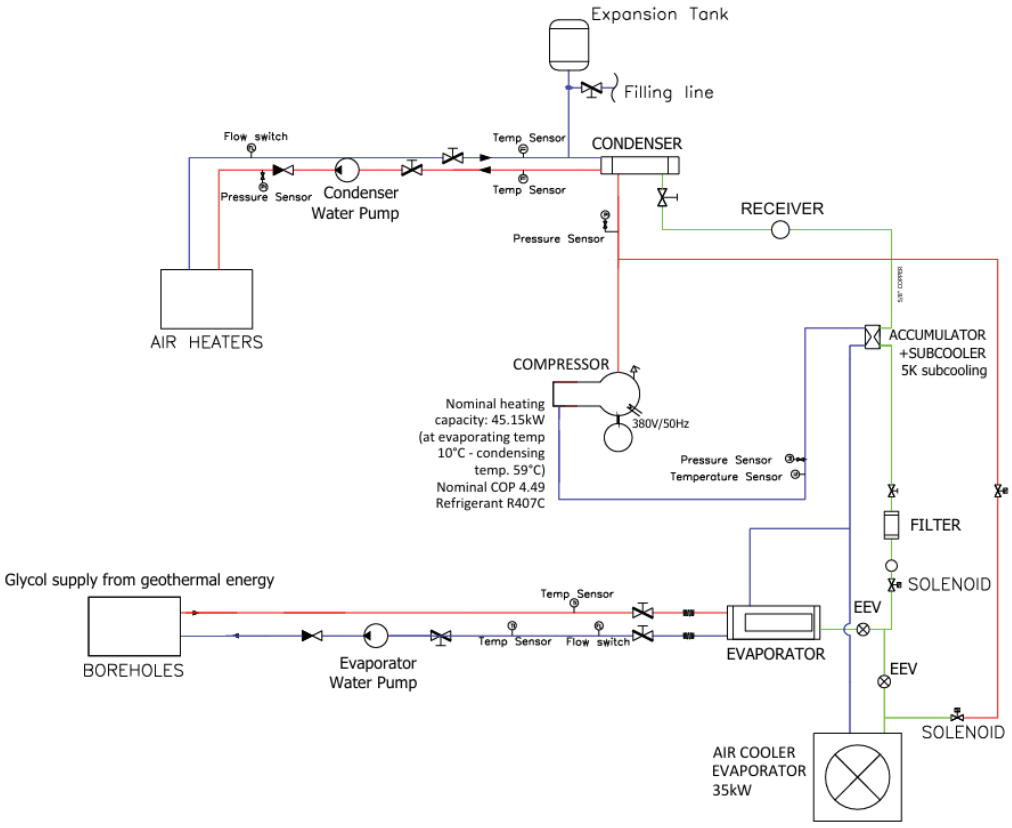

Figure 1: Piping and Instrumentation diagram of the developed heat pump unit.

2.2.1 Heat Exchangers: The multi-source heat pump includes different HEXs, due to their various functions and heat source/sink options. There are three (3) HEXs in total, with the calculations conducted for the refrigerant R407C: one condenser, and two evaporators (an air-heated and a water-heated).

- Plate HEX: The input and output temperatures, as well as the mass flow rates of both sides of each heat exchanger, were the starting point for the sizing. A slight over-surfacing of 6% has been applied to ensure that their performance will be kept within the design conditions over time. The selected plate HEXs are obtained from SWEP, with model B80H, featuring 80 plates and a 4.68 m^2 surface, for the evaporator, and model B85H, with 100 plates and a 5.88 m^2 surface, for the condenser.

https://doi.org/10.52202/077185-0090

- Air-source evaporator: For the design of the evaporator, the type of fin-and-tube HEX was considered, while the calculations were conducted for operating air temperature at 0 °C. The required surface of the heat exchange was 60.12 m^2, and two fans were placed at the back of the unit to facilitate easy installation and to ensure a small pressure drop in the refrigerant circuit.

2.2.2 Digital Scroll Compressor: The selected compressor is the Copeland ZRD 125 KCE5 which is a scroll digital compressor. The compressor is supplied with an external solenoid valve, for achieving capacity modulation. When the solenoid valve is in its normally closed position ("loaded"), the compressor operates at full capacity. When the solenoid valve is energized, the two scroll elements move apart axially ("unloaded"). By varying the time of the "loaded state" and "unloaded state", an average capacity is obtained over the compression cycle (20-second cycle). The main advantage of the scroll digital compressor is that it offers modulation from 10 to 100 %, allowing the system to automatically adjust capacity as needed, while promising 30% more efficient operation than traditional methods of system modulation, according to the manufacturer. The operating envelope of the compressor for the refrigerant R407C has an upper and lower condensation limit of 65 °C and 27 °C respectively, and evaporation temperature ranges from -30 °C to 22 °C.

2.2.3 Miscellaneous Components: The heat pump system also integrates various components to ensure efficient operation and control of the refrigerant cycle, such as electronic expansion valves (EEVs), accumulator, filter, solenoid valves, and hot gas bypass regulator for the defrosting. The schematic diagram of the tested heat pump is shown in Figure 1, with the main components highlighted.

3 METHODOLOGY

The experimental procedure is structured in a way to examine the performance of the heat pump in various operating conditions and capacity loads. For that reason, the unit was initially tested at PSYCTOTHERM's premises, located in Piraeus, Greece, in a modern Heating, Ventilation, and Air Conditioning (HVAC) testing facility, equipped with suitable measuring equipment and auxiliary components, which can efficiently measure and regulate the temperature and flow of the external water circuits, ensuring precise control and accurate data collection.

3.1 Testing Apparatus and Data Acquisition

The two heat exchangers, the condenser, and the evaporator, are connected to the cold and hot water inlets of the testing apparatus, respectively. The laboratory setup is depicted in Figure 2 and two electronically regulated 3-way valves are installed enabling precise control over the mixing of cold and hot water streams.

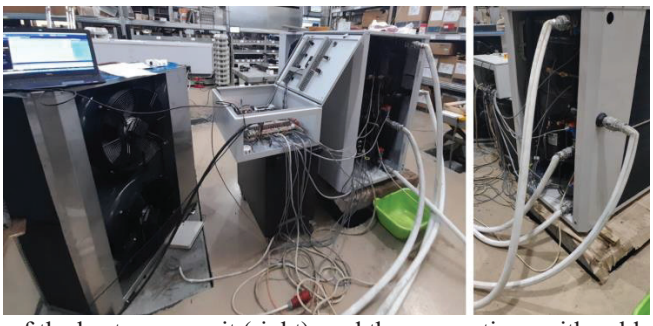

Figure 2: Lab tests of the heat pump unit (right), and the connections with cold and hot water (left).

By adjusting the valve openings from 0% to 100%, desired water temperatures at the evaporator and condenser side of the heat pump can be achieved. Furthermore, by suitable programing of the Programmable Logic Controller (PLC) of the heat pump, the unit can switch between the water-heated, air-heated evaporator, and hybrid operation depending on the heat source availability.

https://doi.org/10.52202/077185-0090

The heat pump and the testing rig are equipped with pressure and temperature sensors, water flow meters, and energy meters, which electronically record the thermodynamic properties of the working fluid and the water circuits. Table 2 lists the main measured key parameters, the processing of which leads to the estimation of the unit's performance and the calculation of the efficiency level.

Table 2: Measuring quantities during the experimental procedure.

Parameter	Symbol (Units)
Electricity consumption of the compressor (net)	$\dot{w}_{comp}$ [kW]
Electricity consumption of the auxiliary parts	$\dot{w}_{aux}$ [kW]
Inlet temperature at the water side of the evaporator	$T_{w,evap,in}$ [°C]
Outlet temperature at the water side of the evaporator	$T_{w,evap,out}$ [°C]
Inlet temperature at the water side of the condenser	$T_{w,cond,in}$ [°C]
Outlet temperature at the water side of the condenser	$T_{w,cond,out}$ [°C]
Refrigerant pressure at the discharge line	$P_{discharge}$ [bar]
Refrigerant pressure at the suction line	$P_{suction}$ [bar]
Water flow at the evaporator side	$\dot{V}_{w,evap}$ [m^3/hr]
Water flow at the condenser side	$\dot{V}_{w,cond}$ [m^3/hr]
Outdoor temperature	$T_{outdoor}$ [°C]

These measurements are collected at a sampling frequency of one (1) second, fully synchronized with other boolean indications from the PLC that define the operational status, such as compressor ON/OFF, water/air operation, defrost operation, etc. All the measurements are recorded in .csv files saved on an SD card within the PLC. In Table 3, the accuracy and measurement range of each sensor is presented.

Table 3: Accuracy of measuring instruments of the installation

Sensor	Quantity	Type	Range	Accuracy
Water flow meter	2	Jumo electromagnetic flow meter	Adjustable	2%
Temperature	5	PT100, 3-wire	0-100 °C	0.1 K
Power meter	2	Janitza UMG 96RM	0-50 kW per phase	0.5%
Refrigerant pressure	2	Pressure transmitter ESCP-MIT1	0-30 bar discharge 0 – 10 bar suction	0.25% of FS

3.2 Performance Calculations

In this section, the basic performance indicators are presented. The processing of experimental measurements was conducted using a numerical model developed in Python for the calculation of water and refrigerant properties. The thermal flows at the condenser and evaporator are identified from the measured data, as it is shown in Equation (1) and Equation (2).

$$\dot{Q}_{cond} = \dot{m}_{w,cond} \cdot c_{p,w,cond}\left(T_{w,cond,out} - T_{w,cond,in}\right) \quad (1)$$

where $c_{p,w,cond}$ $[kJ/kg \cdot K]$ and $\dot{m}_{w,cond}$ $[kg/s]$ are the specific heat under constant pressure and the mass flow rate of the hot source, respectively. The value of $\dot{m}_{w,cond}$ is directly calculated, given the value of $\dot{V}_{w,cond}$ and its density, which is a function of the pressure of the hot source network and the temperature .

The system's COP is calculated according to Equation (2), where $\dot{W}_{HP}$ is the total power consumed by the unit.

$$COP = \frac{\dot{Q}_{cond}}{\dot{W}_{HP}} \quad (2)$$

https://doi.org/10.52202/077185-0090

3.3 SCOP Testing and Calculations

The seasonal performance of a heat pump serves as an indicator of its average efficiency throughout the heating and/or cooling season, considering the diverse energy demands and their fluctuations over time. For the specific application, the SCOP for the water source operation is provided, due to the availability of experimental measurements. To determine the SCOP, the standard methodology which employs spreadsheet calculations is followed, using temperature classes (T_j) and temperature period bins (bin_j) formed by the pairing of outside temperatures (T_j) and the corresponding number of annual hours (h_j). For a more detailed view, the publications of the European Commission (COMMISSION DELEGATED REGULATION (EU), 2013), DIN (DIN, 2013, 2016), and relevant literature (Sieres et al., 2022) give useful information. The SCOP calculation involves defining six testing points based on temperature zones (average, warmer, or colder). In addition to these conditions, measurements are required for the bivalent point (BIV) and the operation limit temperature (TOL). At each measurement point, the HP's coefficient of performance (COP) and heat output are determined. For the case of geothermal heat pumps, these points are simplified to only a single measurement at 10 ºC and a condenser outlet temperature defined by the temperature application, for which the heat pump is tested. Since the COP reflects the HP's performance under full load conditions, a method is employed to integrate part-load behavior. According to EN 14825 (DIN, 2016) for a water-sink HP, the COP at part load conditions is given according to Equation (3).

$$COP_{PL} = COP_{DC} \cdot \frac{CR}{C_c \cdot CR + (1 - C_c)} \tag{3}$$

where the part load factor (capacity ratio) CR is the quotient of the heat demand and the heating capacity at full load and the degradation coefficient C_c is set to 0.9 (DIN, 2016). The heat demand is determined based on the outdoor temperature class T_j according to Equation (4), which represents the part load ratio at different test temperatures, defined by Equation (5).

$$\dot{Q}_h(T_j) = Pdesign_h\% \cdot \dot{Q}_h(T_{design}) \tag{4}$$

$$Pdesign_h\% = \frac{T_j - 16}{T_{design} - 16} \tag{5}$$

where $\dot{Q}_h(T_{design})$ is the nominal heat load at the design temperature T_{design}, which for average climate conditions is set to -10 ºC.

In addition, for temperatures below the bivalent temperature, the thermal output of the heat pump is not sufficient to cover the load, and an additional heater is used with COP=1 by the definition. As a result, the COPs at part load conditions and the heating capacity are then suitably inter - and extrapolated to cover all temperature classes.

For the overall efficiency, the ratio of the total covered heat load and total electricity consumption is identified as the average seasonal efficiency of the heat pump in active mode (Equation (6)).

$$SCOP_{on} = \frac{\sum_j \dot{Q}_h(T_j)}{\sum_j \dot{W}_{HP,PL}(T_j)} \tag{6}$$

where $\dot{W}_{HP,PL}(T_j)$ is the total electricity demand at every temperature bin (T_j) determined by the COP at part load conditions. Therefore, the last step includes the calculation of the overall SCOP, in which the heat pump's consumption when deactivated must be included (Equation (7)). This includes the electricity consumption at thermostat off mode (subscript TO), standby mode (subscript SB), crankcase heater mode (subscript CK), and off mode (subscript OFF). Specifically, off mode and crankcase heater mode have zero electricity consumption, while standby mode and thermostat off mode consume 15 W each. After all, the calculation of the SCOP is determined according to Equation (7):

$$SCOP = \frac{\sum_j \dot{Q}_h(T_j)}{\frac{\sum_j \dot{Q}_h(T_j)}{SCOP_{on}} + H_{TO} \cdot E_{TO} + H_{SB} \cdot E_{SB} + H_{CK} \cdot E_{CK} + H_{OFF} \cdot E_{OFF}} \tag{7}$$

https://doi.org/10.52202/077185-0090

where H signifies the number of hours in a year the heat pump is in the stated operating mode. Both the number of hours H and each power consumption E is defined according to (DIN, 2016).

4 RESULTS AND DISCUSSION

4.1 Heat Pump Performance for Varying Capacity Under Different Operation Modes

During the experimental procedure, the measurements are collected at intervals of 1 second. Subsequently, the average values over a 20-second period are computed to align with the operational cycle of the digital capacity modulation. Taking into consideration the analysis provided in Section 3, the heat pump's performance under different operation modes (water- and air-source) is presented. The water temperatures at the evaporator's inlet vary between 8 and 20 °C, while at the condenser, the outlet water temperature ranges from 30 to 50 °C. Figure 3 depicts the heating capacity of the heat pump and the electrical consumption as a function of the compressor's pressure ratio, while Figure 4 illustrates the COP variation with the refrigerant pressure ratio at different capacities of the compressor. Observations indicate that at 100% compressor capacity, the available measurements are approaching pressure ratios slightly exceeding 4, leading to a heating capacity of approximately 30-32 kW, and associated electrical consumption of 6 kW_e, resulting in a COP of about 5. As capacities decrease, the corresponding pressure ratio also decreases, leading to a reduction in thermal load and electricity consumption. Operating at 80% capacity results in a lower electric power demand, consequently yielding a higher COP for pressure ratios around 3. For the same pressure ratios as 100% capacity, operating at 80% capacity is expected to produce a heating capacity of 25 kW (a 16% reduction) with a COP close to 4, according to the measurements. For the operation at 60% and 20%, there is a notable reduction of over 40% and 65% respectively in heating capacity, leading to an average COP of 4.2 for both cases, in pressure ratios of around 3. Furthermore, during digital capacity operation at 20%, where compression occurs only for four (4) seconds within the 20-second cycle, heating capacity, and electricity consumption remain relatively constant across the entire operational spectrum.

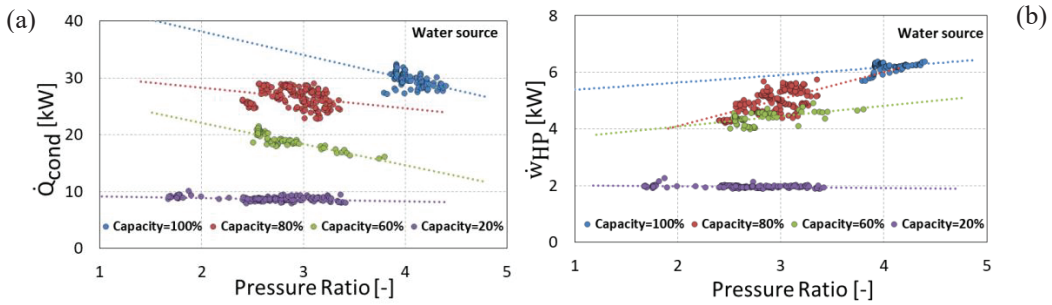

Figure 3: Heating capacity (a) and electric power (b) of the water-source mode in different capacities, as a function of the pressure ratio.

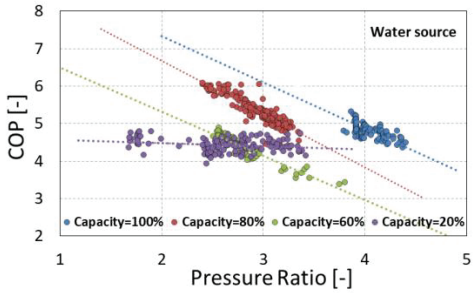

Figure 4: COP of the water-source mode in different capacities, as a function of the pressure ratio.

Figure 5 and Figure 6, present the same graphs for the air-source mode, showing the unit's heating capacity, electric power, and COP as the pressure ratio varies. The tests were conducted with outdoor temperatures ranging between 16-20 °C and varying the water outlet at the condenser between 30 – 50

https://doi.org/10.52202/077185-0090

ºC. When the compressor operates at 100% capacity for a pressure ratio between 3 to 6, the unit's heating capacity exceeds 30 kW. For the same operating conditions, the electric consumption was measured at about 7-12 kW_e, leading to a COP in the range of 3-4. It is observed that for a capacity of 80%, the electric consumption is higher, probably due to the abrupt increase of the fan's consumption far from the design point. Under similar conditions, operation at 60% and 20% of full capacity exhibits a similar trend to the water option concerning the heating capacity. For electricity consumption, an increase of 1.5 – 2 kW is observed, thereby negatively impacting the COP.

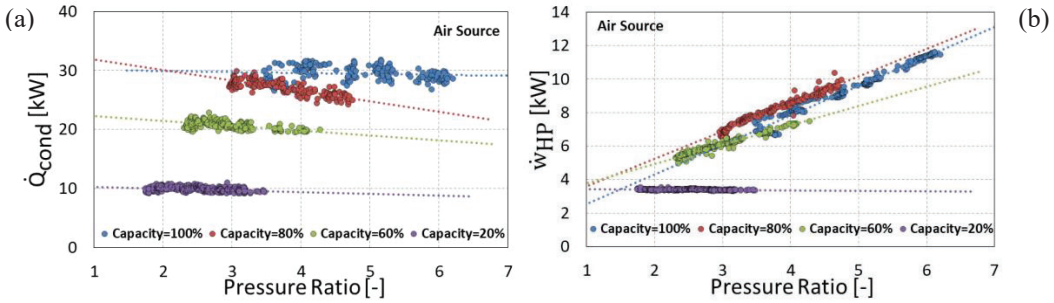

Figure 5: Heating capacity (a) and electric power (b) of the air-source mode in different capacities, as a function of the pressure ratio.

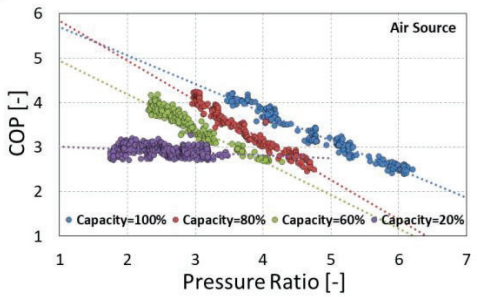

Figure 6: COP of the air-source mode in different capacities, as a function of the pressure ratio.

Finally, the heating capacity, electric power, and COP for the water-source, air-source, and hybrid mode are visually represented in Figure 7 and Figure 8. The air-source system was subjected to testing in early June when the ambient air temperature was above 15 ºC. This choice of testing conditions highlights the modest enhancement in COP achieving a maximum value of 4.5 in hybrid mode compared to 4.1 in air source at pressure ratio of 3.7. The highest COP improvement, up to 10%, is observed at lower pressure ratios, where the heating capacity is significantly enhanced. The rationale behind this lies in the fact that, under typical operational circumstances, the hybrid mode is engaged in conditions of lower air temperatures, typically ranging from approximately 5 to 10 °C. Also, the electrical power consumed for hybrid operation is higher since both fans and water pumps are enabled, leading to increased energy consumption, and offering the highest possible thermal capacity to the building. As expected, the water-source operation leads to the highest COP performance compared to the air-source and hybrid modes, as the water temperature is higher than the corresponding air temperatures. The tests for the water-source mode present a limited pressure ratio range, as the water's hot and cold sides do not vary as significantly as the air during testing. On the other hand, despite the weak COP enhancement, hybrid operation significantly improves the heating capacity of the system, resulting in an almost 8 kW_{th} increment for the same conditions, compared to the other two modes. Based on these findings, it is evident that water source operation demonstrates a higher COP, and this highlights the importance of favoring this mode alongside hybrid mode, to maximize the system's overall performance during field operations.

https://doi.org/10.52202/077185-0090

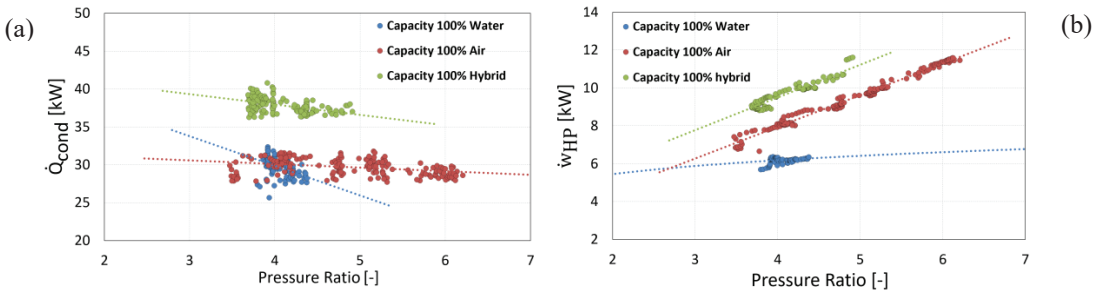

Figure 7: Heating capacity (a) and electric power (b) in 100% compressor capacity, as a function of the pressure ratio, for the three different operation scenarios.

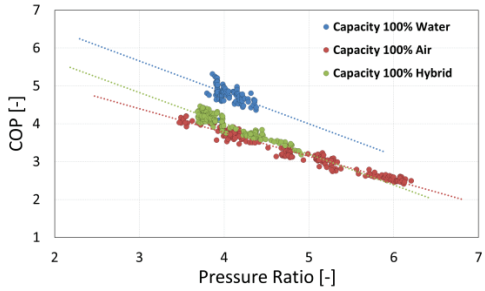

Figure 8: COP in 100% compressor capacity, as a function of the pressure ratio, for the three different operation scenarios.

4.2 Seasonal COP Evaluation

In this section, the results of the SCOP calculations for the water source mode of the heat pump are presented, according to the European Standard EN 14825 (DIN, 2016). In the European energy labelling, SCOP for the Average climate profile is mandatory and for that reason, the seasonal HP performance is identified based on that specific profile. The climate zone base for the "Average" profile is the temperature distribution of Strasbourg with a total heating season of 4910 hours. The design temperature for the chosen climate zone is -10 ºC with the heating demand adjusted to the installation's specific thermal requirements. The SCOP calculations focus on "Medium" temperature applications with the part load test conditions corresponding to a single testing point at 10 °C outdoor HEX temperature and 45 °C indoor HEX temperature (DIN, 2016). The heat pump is equipped with constant flow water circulators maintaining a consistent outlet temperature for all conditions, with water flow rates determined according to EN14511 standard (DIN, 2013). The operational limit and bivalent temperature of the heat pump are set at -10 °C and -9 °C, respectively. The Seasonal Coefficient of Performance (SCOP) is shown in Table 4, while Figure 9 illustrates the heating load curve, the heating capacity of the HP, and the COP at part load conditions as a function of the outdoor temperature. The results in Figure 9 indicate that the HP can meet the heat demand across nearly the entire range of outdoor temperatures. However, when outdoor temperatures exceed 12 °C, the demand falls below the compressor's minimum capacity. Consequently, the heating capacity remains constant at this minimum level, leading to a decrease in COP by up to 7%, attributed to the degradation factor when operating with a capacity ratio below 1.

Table 4: SCOP for the water source mode of the heat pump

Reference heating season		**"A" Average**	
Seasonal Efficiency	Reference Heating Season (EN14824), Medium temperatures (Fixed outlet 45 ºC)	Pdesign, kW	33.38
		SCOPon	4.09
		SCOP	4.08

https://doi.org/10.52202/077185-0090

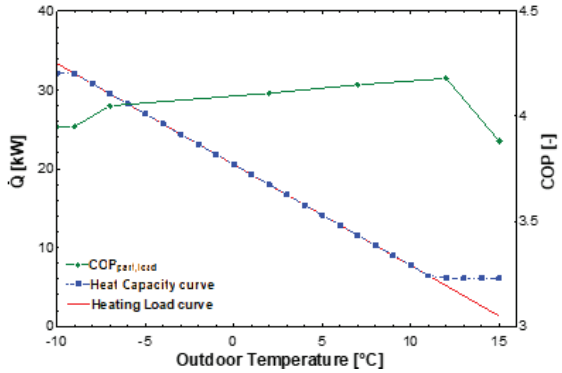

Figure 9: Heating load curve, heat capacity curve, and part load COP of the heat pump as a function of the outdoor temperature.

4.3 Digital Capacity Operation

Compressor capacity modulation can reduce energy consumption and control the HP's performance as was described in section 2.2. When the compressor is operating in loaded mode the compressor behaves like a standard scroll compressor providing 100% capacity. Figure 10 illustrates the heat pump's operation with capacity control enabled (at 80% and 60%) over a 2-minute sample period. In Figure 10(a), the electricity consumption of the compressor is depicted, revealing distinct cycle timing differences between the two capacity modes. During unloaded phases, electricity consumption drops to approximately 2 kW. In contrast, during loaded phases, both 80% and 100% capacity modes exhibit similar consumption levels, whereas the 60% operation shows a 3-4% reduction in electricity consumption. Figure 10(b) showcases heating capacity variations, highlighting a notable 10 kW disparity between the 80% and 60% modes during compressor unloaded phases. The main reason for this variance is that longer compressor operation leads to elevating refrigerant temperatures and subsequently increased water temperatures and heating capacities. Regarding the refrigerant pressure, during the loading phase, the operating pressure ratio in 80% capacity is higher compared to 60% mode, leading to 2-5 bar higher pressure at the discharge line (Figure 10(c)) and 0.5 – 1.5 lower pressure at the suction (Figure 10(d)).

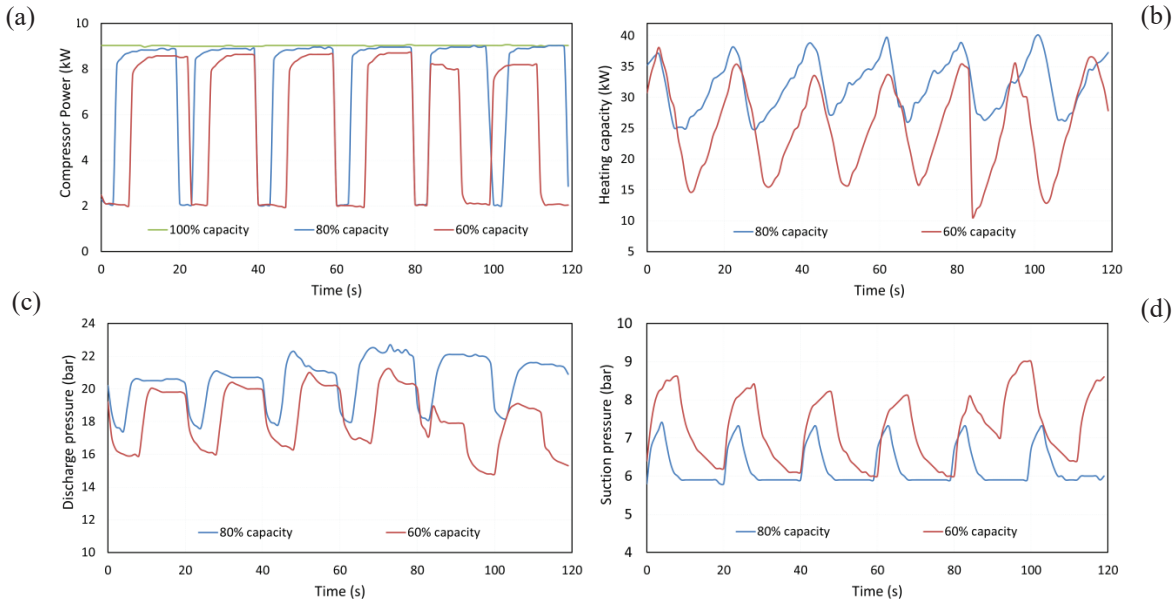

Figure 10: Heat pump operation with enabled capacity control (80% and 60%) during a sample of 2 minutes: (a) Power, (b) Heating capacity, (c) Suction pressure of the compressor, (d) Discharge pressure of the compressor.

https://doi.org/10.52202/077185-0090

5 CONCLUSIONS

In conclusion, this research focuses on an experimental evaluation of a DSHP with digital capacity modulation, specifically designed for swine nursery barns. The key characteristics and components of the system are provided, and the HP's performance is evaluated over a range of temperatures and capacities including air source, water source, and hybrid mode operation. Results indicate that at full compressor capacity, the water source operation achieves a heating capacity of 30-32 kW with a COP of around 5, while air source operation yields over 30 kW heating capacity with 7-12 kW electric consumption and a COP of 3-4. Decreasing compressor capacity leads to reduced thermal output by up to 65%, in order to achieve better compliance with the building's thermal needs. Hybrid operation demonstrates enhanced heating capacity compared to the other two modes but with higher energy consumption. Despite the higher heating capacity in hybrid mode, water-source operation outperforms in terms of COP by approximately 15%. In addition, special focus is given to the calculation of HP's SCOP in accordance with EN 14825. The SCOP calculations are based on "Medium" temperature applications for the "Average" climate zone, revealing a SCOP= 4.08 for ground source HP operation. Finally, the dynamic performance of the digital capacity control is highlighted, illustrating the performance of the system over a period of 120 seconds for 80 % and 60 % capacity. The impact of digital capacity modulation reveals variances in electricity consumption and heating capacity, with longer compressor operation leading to higher pressure ratios and discharge pressures. This comprehensive analysis offers valuable insights into the performance of DSHPs for livestock environments, enhancing operational efficiency and versatility in heating systems.

NOMENCLATURE

C_c	degradation coefficient
c_p	specific heat under constant pressure
COP	coefficient of performance
CR	capacity ratio
E	power consumption
H	number of hours
$\dot{m}$	mass flow rate
P	pressure
$Pdesign_h$	part Load Ratio
$\dot{Q}$	heat flow
SCOP	seasonal coefficient of performance
T	temperature
$\dot{V}$	volume flow rate
$\dot{w}$	electrical power

Subscript

aux	auxiliary consumption
CK	crankcase heater
comp	compressor
cond	condenser
discharge	discharge line
DC	declared capacity
design	design point
evap	evaporator
h	heating
HP	heat pump
j	temperature class
off	off mode
on	active mode

https://doi.org/10.52202/077185-0090

outdoor	outdoor conditions
PL	part load
SB	stand-by mode
duction	suction line
TO	thermostat-off mode
w	water

REFERENCES

COMMISSION DELEGATED REGULATION (EU). (2013). *supplementing Directive 2010/30/EU of the European Parliament and of the Council with regard to the energy labelling of water heaters, hot water storage tanks and packages of water heater and solar device. No 812/2013*.

Corberán, J. M., Cazorla-Marín, A., Marchante-Avellaneda, J., & Montagud, C. (2018). Dual source heat pump, a high efficiency and cost-effective alternative for heating, cooling and DHW production. *International Journal of Low-Carbon Technologies*, *13*(2), 161–176. https://doi.org/10.1093/ijlct/cty008

DIN. (2013). *DIN EN14511-1:2015-12, Air Conditioners, Liquid Chilling Packages and Heat Pumps for Space Heating and Cooling and Process Chillers Using Electrically Driven Compressors*.

DIN. (2016). *DIN EN 14825:2016-10, Air Conditioners, Liquid Chilling Packages and Heat Pumps, with Electrically Driven Compressors, for Space Heating and Cooling Testing and Rating at Part Load Conditions and Calculation of Seasonal Performance*.

Grossi, I., Dongellini, M., Piazzi, A., & Morini, G. L. (2018). Dynamic modelling and energy performance analysis of an innovative dual-source heat pump system. *Applied Thermal Engineering*, *142*, 745–759. https://doi.org/10.1016/j.applthermaleng.2018.07.022

Han, Z., Ju, X., Qu, L., Liu, J., Ma, X., & Zhang, S. (2017). Experimental study of the performance of a double-source heat-pipe composite vapour-compression heating unit. *Solar Energy*, *155*, 1208–1215. https://doi.org/10.1016/j.solener.2017.07.062

Li, Y., Cui, Y., Song, Z., Zhao, X., Li, J., & Shen, C. (2023). Eco-economic performance and application potential of a novel dual-source heat pump heating system. *Energy*, *283*, 128478. https://doi.org/10.1016/j.energy.2023.128478

Marinelli, S., Lolli, F., Butturi, M. A., Rimini, B., & Gamberini, R. (2020). Environmental performance analysis of a dual-source heat pump system. *Energy and Buildings*, *223*, 110180. https://doi.org/10.1016/j.enbuild.2020.110180

Meramveliotakis, G., Kosmadakis, G., Krikas, A., Gomes, J., & Pilou, M. (2020). Innovative Coupling of PVT Collectors with Electric-Driven Heat Pumps for Sustainable Buildings. *Proceedings of the ISES EuroSun 2020 Conference – 13th International Conference on Solar Energy for Buildings and Industry*, 1–12. https://doi.org/10.18086/eurosun.2020.05.01

Pilou, M., Kosmadakis, G., & Meramveliotakis, G. (2023). Modeling of an Integrated Renewable-Energy-Based System for Heating, Cooling, and Electricity for Buildings. *Energies*, *16*(12), 4691. https://doi.org/10.3390/en16124691

Sieres, J., Ortega, I., Cerdeira, F., Álvarez, E., & Santos, J. M. (2022). Seasonal Efficiency of a Brine-to-Water Heat Pump with Different Control Options according to Ecodesign Standards. *Clean Technologies*, *4*(2), 542–554. https://doi.org/10.3390/cleantechnol4020033

Wang, Y., Quan, Z., Jing, H., Wang, L., & Zhao, Y. (2021). Performance and operation strategy optimization of a new dual-source building energy supply system with heat pumps and energy storage. *Energy Conversion and Management*, *239*, 114204. https://doi.org/10.1016/j.enconman.2021.114204

ACKNOWLEDGEMENT

This study was developed in the framework of the Horizon 2020 RES4LIVE: "Energy Smart Livestock Farming towards Zero Fossil Fuel Consumption" project (www.res4live.eu) funded by the European Commission (Grant agreement No.101000785).

https://doi.org/10.52202/077185-0090